Electronic Supplementary Material (ESI) for Dalton Transactions.

Supporting online information for

Amphoteric reactivity of a putative Cu(II)-*m*CPBA intermediate‡

Rakesh Kumar, Anweshika Maji, Bhargab Biswas, and Apparao Draksharapu*

Southern Laboratories - 208A, Department of Chemistry, Indian Institute of Technology Kanpur, Kanpur-208016 (India).
appud@iitk.ac.in

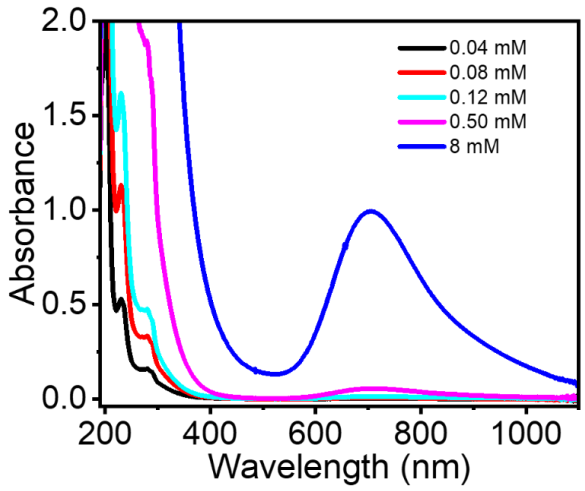

Figure S1: UV/Vis absorption spectra at different concentration (black) 0.04 mM, (red) 0.08 mM, (cyan) 0.12 mM, (magenta) 0.50 mM, and (blue) 8 mM of **1**.

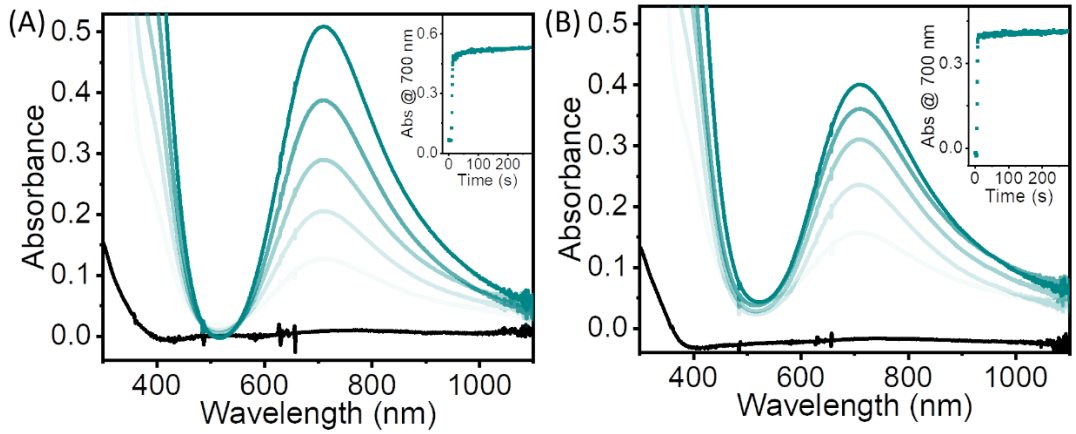

Figure S2: UV/Vis absorption changes upon reaction of (A) 3 equivalents and (B) 10 equivalents of *m*CPBA with 8 mM $[Cu^{I}(NCCH_3)_4](ClO_4)$ in CH_3CN at 25 ^{o}C. Inset: The corresponding changes in the absorption at 700 nm over time in seconds.

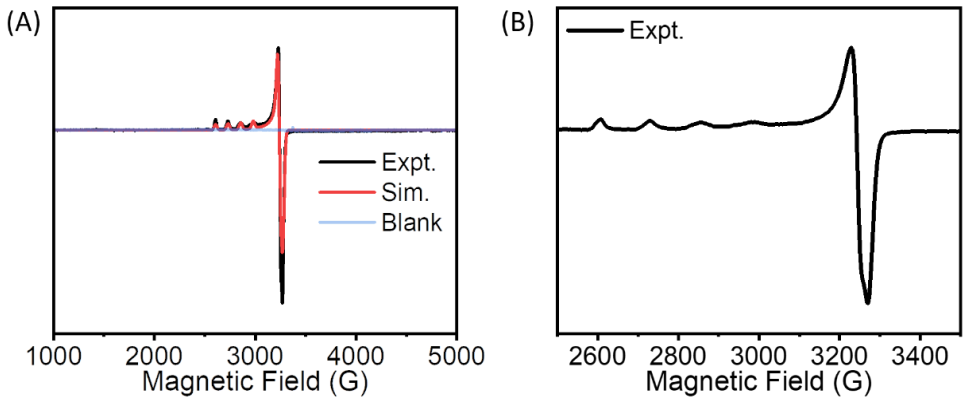

Figure S3: (A) Experimental (black) and simulated (red) X-band EPR spectra of **1** ($g_x = g_y = 2.08$, $g_z = 2.41$; $A_x = A_y = 0$ G, $A_z = 130$ G), and (blue) $[Cu^{I}(NCCH_3)_4](ClO_4)$ (B) Zoomed in experimental spectrum of **1** measured at 120 K; modulation amplitude 2.08 G; modulation frequency 100 kHz, and attenuation 20 dB. *Condition to generate **1**: 2 mM $[Cu^{I}(NCCH_3)_4](ClO_4)$ in CH_3CN treated with 1 eq. of mCPBA at 25 ^{o}C.*

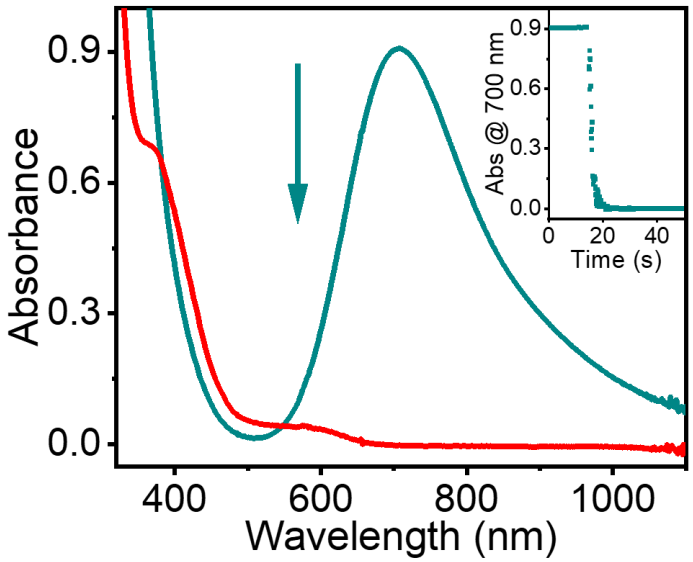

Figure S4: UV/Vis absorption changes depicting the reaction of 8 mM **1** with 20 eq. of *p*-cresol at 25 ^{o}C. Inset: The corresponding changes in the absorption at 700 nm over time in seconds. *Conditions to generate **1**: 8 mM [Cu^{I}(NCCH$_3$)$_4$](ClO$_4$) in CH$_3$CN + 1 eq. of mCPBA at 25 ^{o}C.*

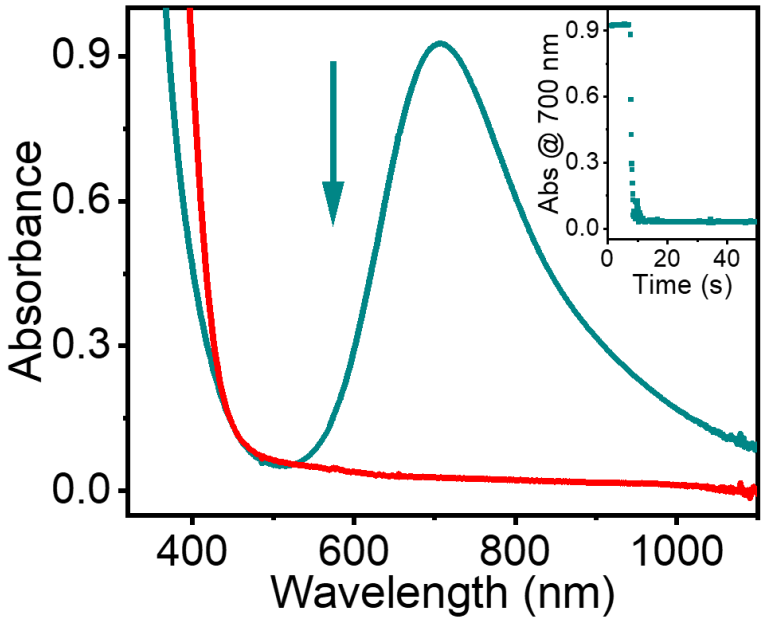

Figure S5: UV/Vis absorption changes depicting the reaction of 8 mM **1** with 20 eq. of *p*-fluorophenol at 25 ^{o}C. Inset: The corresponding changes in the absorption at 700 nm over time in seconds. *Conditions to generate **1**: 8 mM [Cu^{I}(NCCH$_3$)$_4$](ClO$_4$) in CH$_3$CN + 1 eq. of mCPBA at 25 ^{o}C.*

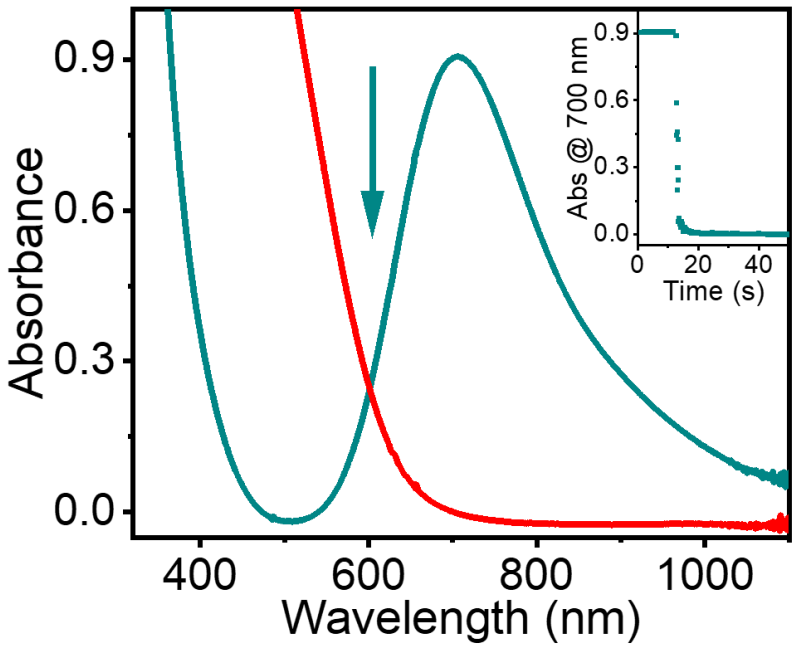

Figure S6: UV/Vis absorption changes depicting the reaction of 8 mM **1** with 20 eq. of phenol at 25 ^{o}C. Inset: The corresponding changes in the absorption at 700 nm over time in seconds. *Conditions to generate **1**: 8 mM [Cu^{I}(NCCH$_3$)$_4$](ClO$_4$) in CH$_3$CN + 1 eq. of mCPBA at 25 ^{o}C.*

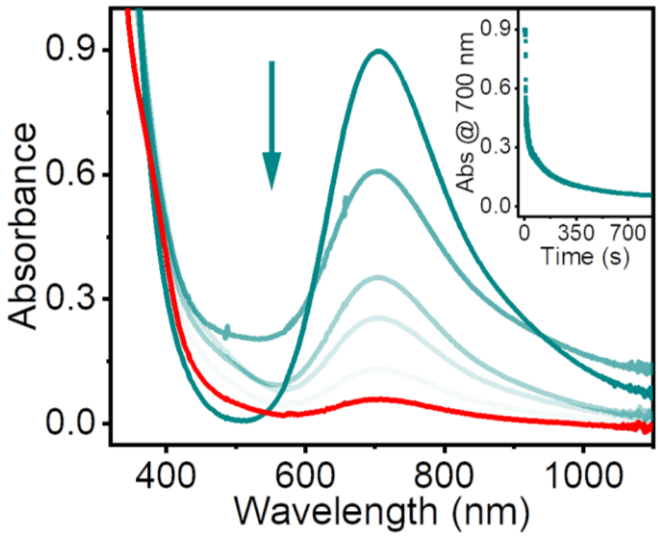

Figure S7: UV/Vis absorption changes depicting the reaction of 8 mM **1** with 20 eq. of *p*-hydroxybenzonitrile at 25 ^{o}C. Inset: The corresponding changes in the absorption at 700 nm over time in seconds. *Conditions to generate **1**: 8 mM [Cu^{I}(NCCH$_3$)$_4$](ClO$_4$) in CH$_3$CN + 1 eq. of mCPBA at 25 ^{o}C.*

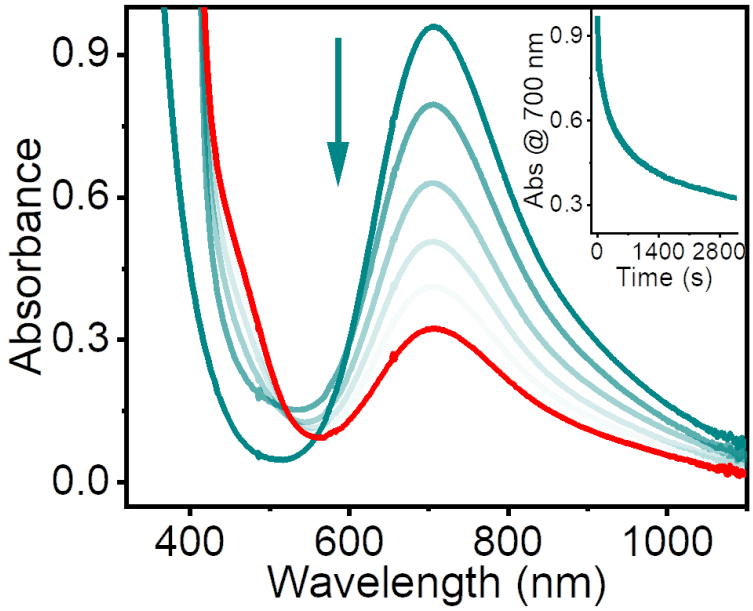

Figure S8: UV/Vis absorption changes depicting the reaction of 8 mM **1** with 20 eq. of *p*-nitrophenol at 25 ^{o}C. Inset: The corresponding changes in the absorption at 700 nm over time in seconds. *Conditions to generate **1**: 8 mM [Cu^{I}(NCCH$_3$)$_4$](ClO$_4$) in CH$_3$CN + 1 eq. of mCPBA at 25 ^{o}C.*

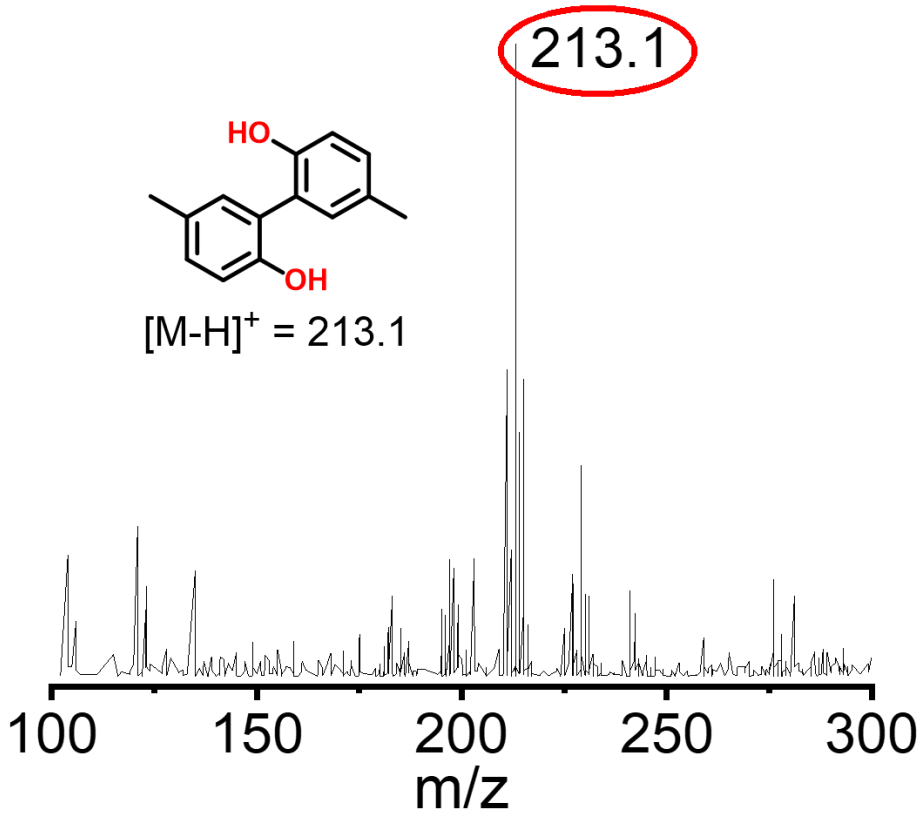

Figure S9: Product analysis of the reaction of **1** with 2 eq. of *p*-cresol by ESI-MS. *Conditions to generate **1**: 20 mM [Cu^{I}(NCCH$_3$)$_4$](ClO$_4$) in CH$_3$CN + 1 eq. mCPBA at 25 ^{o}C.*

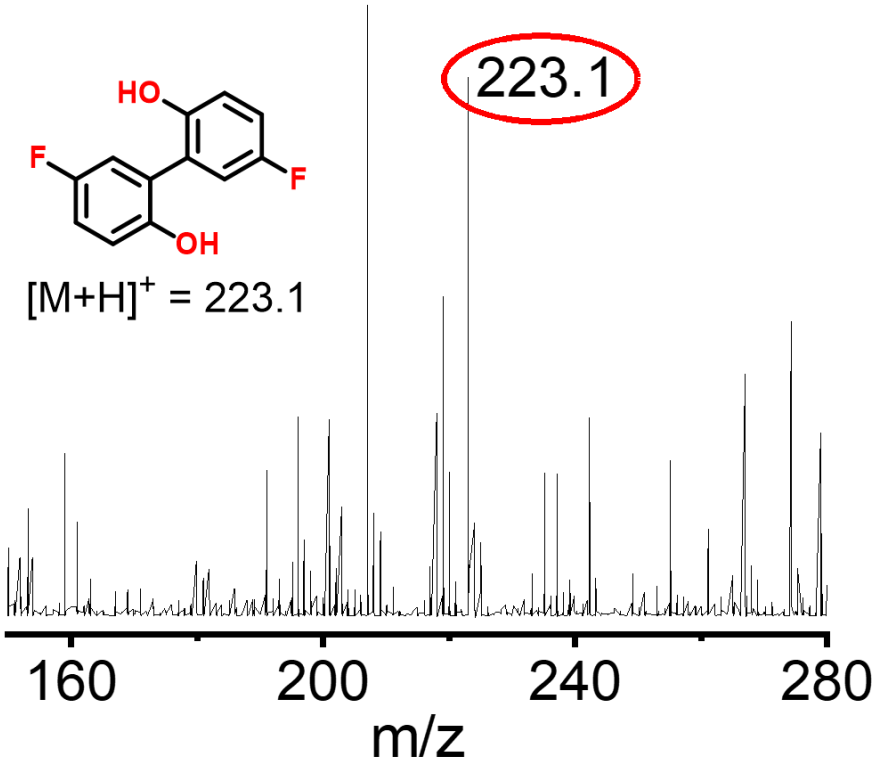

Figure S10: Product analysis of the reaction of **1** with 2 eq. of *p*-flurophenol by ESI-MS. *Conditions to generate **1**: 20 mM [Cu^{I}(NCCH$_3$)$_4$](ClO$_4$) in CH$_3$CN + 1 eq. mCPBA at 25 ^{o}C.*

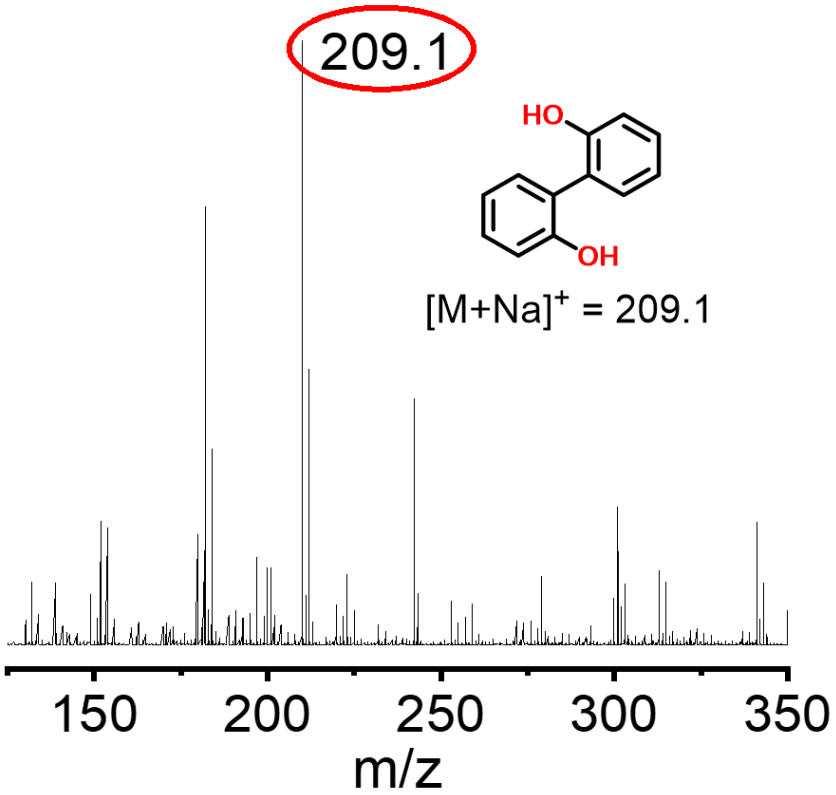

Figure S11: Product analysis of the reaction of **1** with 2 eq. of phenol by ESI-MS. *Conditions to generate **1**: 20 mM [Cu^{I}(NCCH$_3$)$_4$](ClO$_4$) in CH$_3$CN + 1 eq. mCPBA at 25 ^{o}C.*

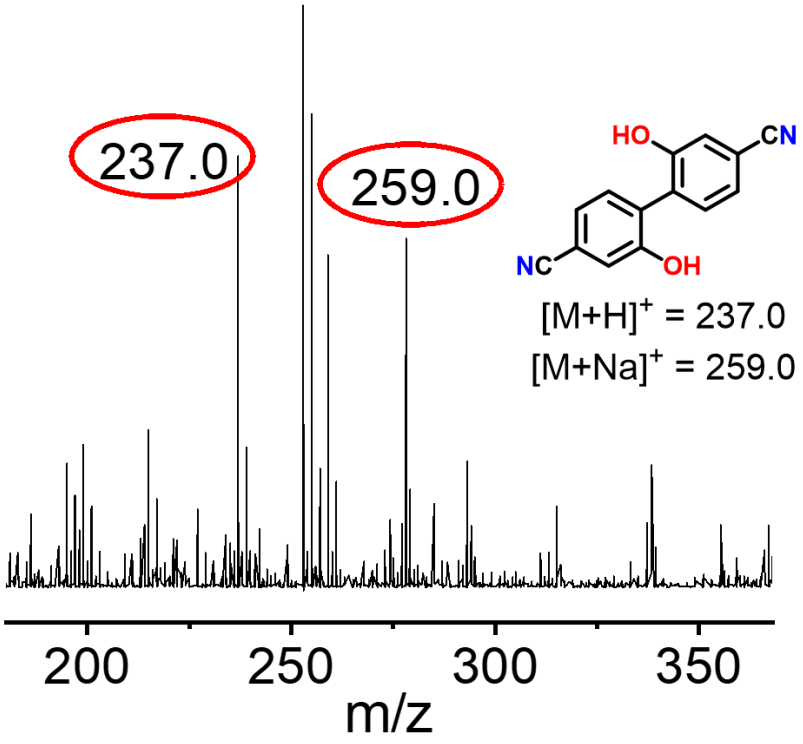

Figure S12: Product analysis of the reaction of **1** with 2 eq. of *p*-hydroxybenzonitrile by ESI-MS. *Conditions to generate **1**: 20 mM [Cu^{I}(NCCH$_3$)$_4$](ClO$_4$) in CH$_3$CN + 1 eq. mCPBA at 25 ^{o}C.*

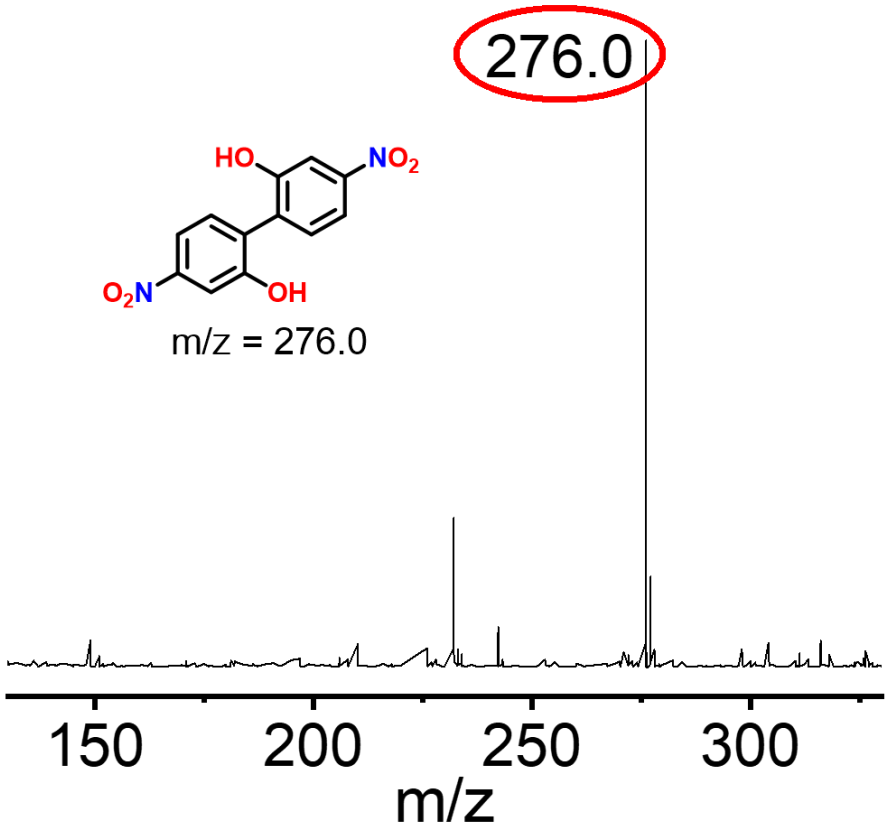

Figure S13: Product analysis of the reaction of **1** with 100 eq. of *p*-nitro phenol by ESI-MS. *Conditions to generate **1**: 20 mM [Cu^{I}(NCCH$_3$)$_4$](ClO$_4$) in CH$_3$CN + 1 eq. mCPBA at 25 ^{o}C.*

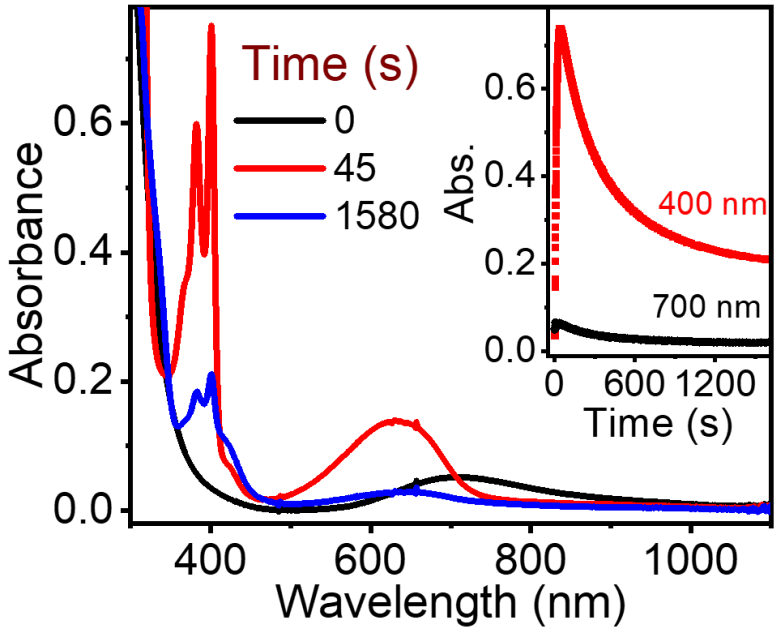

Figure S14: UV/Vis absorption changes depicting the reaction of 0.5 mM **1** with 2 eq. of 2,4,6-TTBP. Inset: The corresponding changes in the absorption at 400 nm (red) and 700 (black) nm over time in seconds. *Conditions to generate **1**: 0.5 mM [Cu^{I}(NCCH$_3$)$_4$](ClO$_4$) in CH$_3$CN + 1 eq. of mCPBA at 25 ^{o}C.*

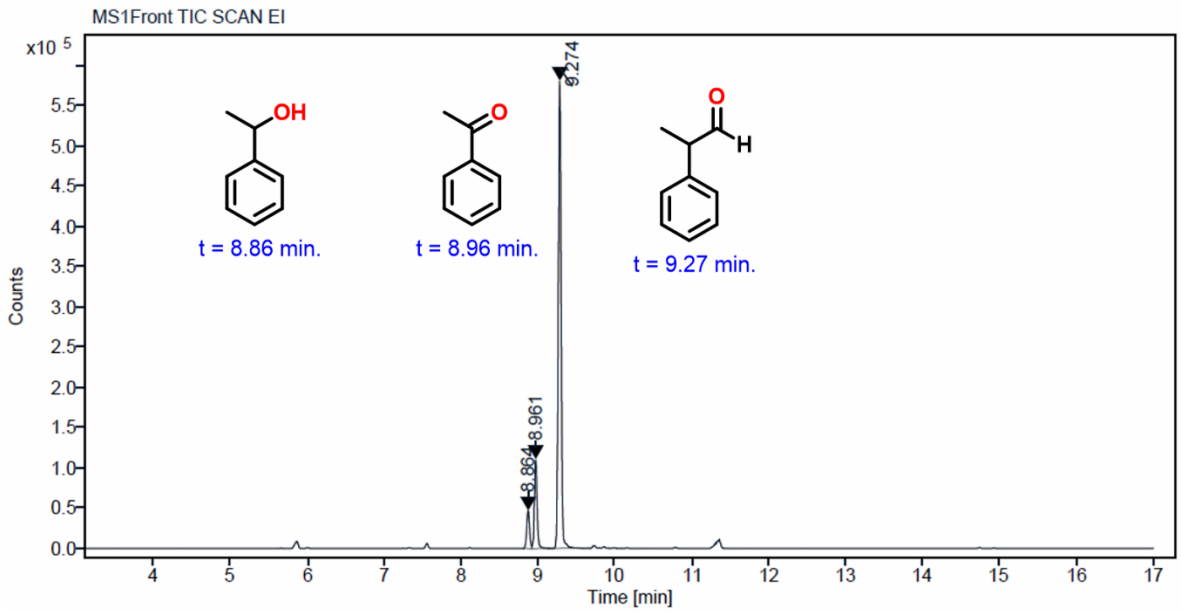

Figure S15: Gas Chromatogram of the reaction of **1** with 5 eq. of 2-PPA at 40 ^{o}C. *Conditions to generate **1**: 20 mM [Cu^{I}(NCCH$_3$)$_4$](ClO$_4$) in CH$_3$CN + 1 eq. mCPBA at 25 ^{o}C.*

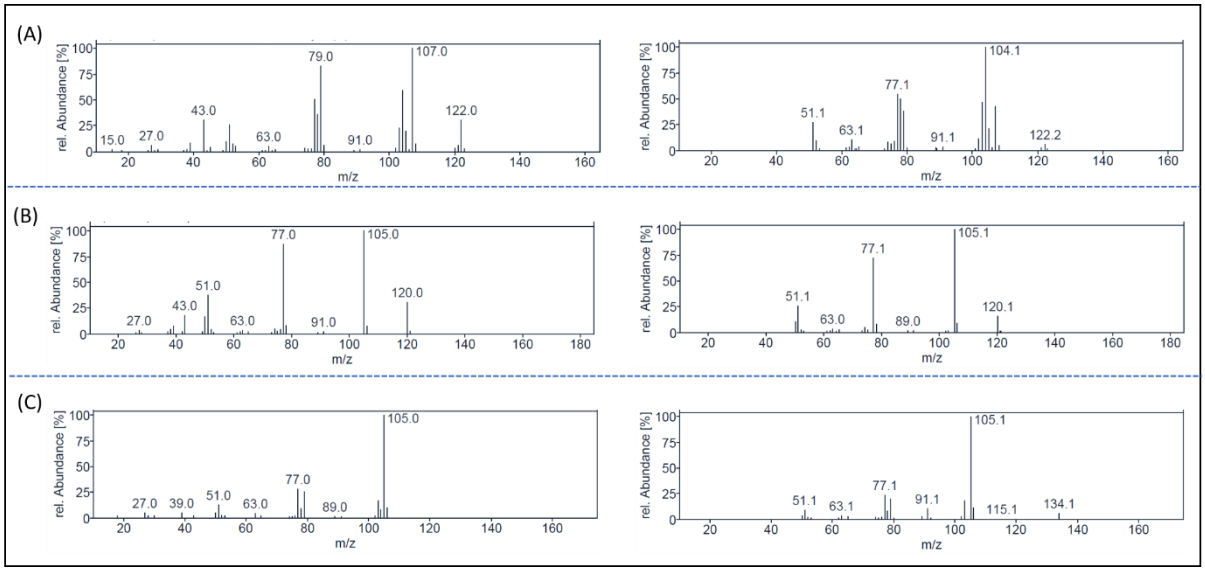

Figure S16: Product analysis of the reaction of **1** with 5 eq. of 2-PPA at 40 ^{o}C by GC followed by mass spectrometry. (Left) Experimental mass fragment data with peaks at corresponding retention time (in min.) (A) 8.862 min. for 1-phenylethanol (B) 8.959 min. for acetophenone, and (C) 9.274 min. for 2-PPA; (Right) simulated from the mass library of GCMS. *Conditions to generate **1**: 20 mM [Cu^{I}(NCCH$_3$)$_4$](ClO$_4$) in CH$_3$CN + 1 eq. mCPBA at 25 ^{o}C.*

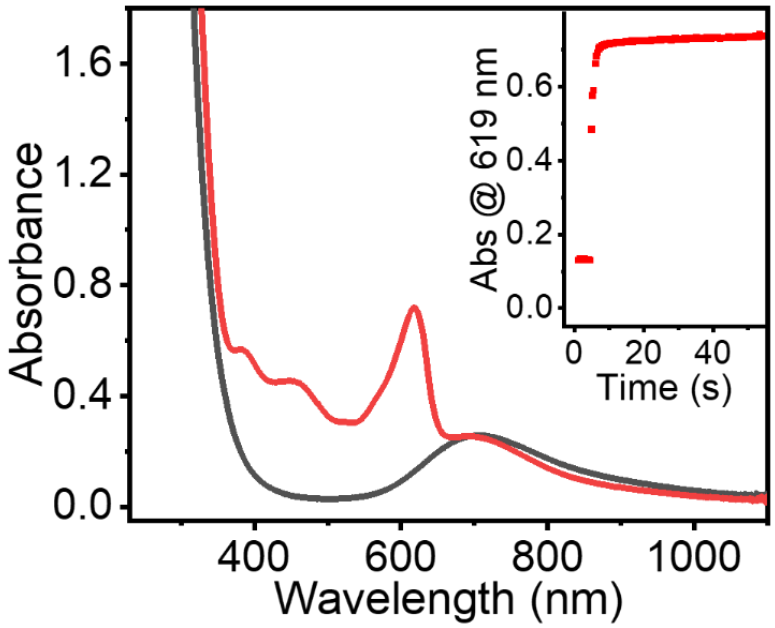

Figure S17: UV/Vis absorption changes depicting the reaction of 2 mM **1** with 2 eq. of ferrocene. Inset: The corresponding changes in the absorption at 619 nm due to ferrocenium (Fc^{+}) over time in seconds. *Conditions to generate **1**: 2 mM [Cu^{I}(NCCH$_3$)$_4$](ClO$_4$) in CH$_3$CN + 1 eq. of mCPBA at 25 ^{o}C.*

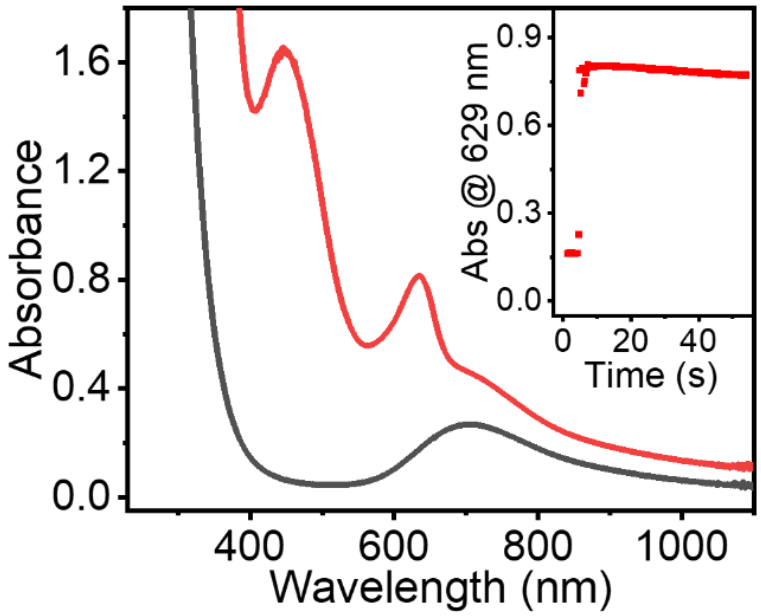

Figure S18: UV/Vis absorption changes depicting the reaction of 2 mM **1** with 2 eq. of acetylferrocene. Inset: The corresponding changes in the absorption at 629 nm due to acetylferrocenium ($AcFc^+$) over time in seconds. *Conditions to generate **1**: 2 mM $[Cu^I(NCCH_3)_4](ClO_4)$ in CH_3CN + 1 eq. mCPBA at 25 ^oC.*

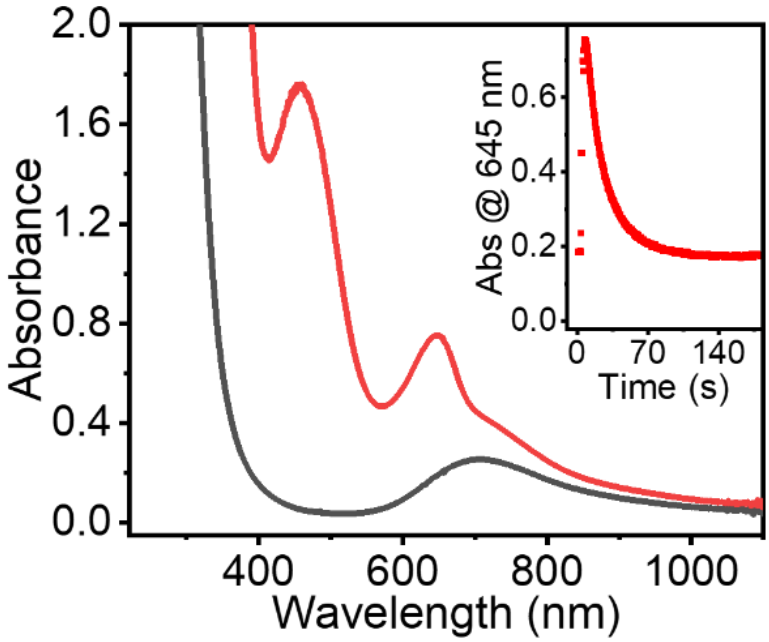

Figure S19: UV/Vis absorption changes depicting the reaction of 2 mM **1** with 2 eq. of diacetyl ferrocene. Inset: The corresponding changes in the absorption at 645 nm due to diacetylferrocenium (Ac_2Fc^+) over time in seconds. *Conditions to generate **1**: 2 mM $[Cu^I(NCCH_3)_4](ClO_4)$ in CH_3CN + 1 eq. mCPBA at 25 ^oC.*

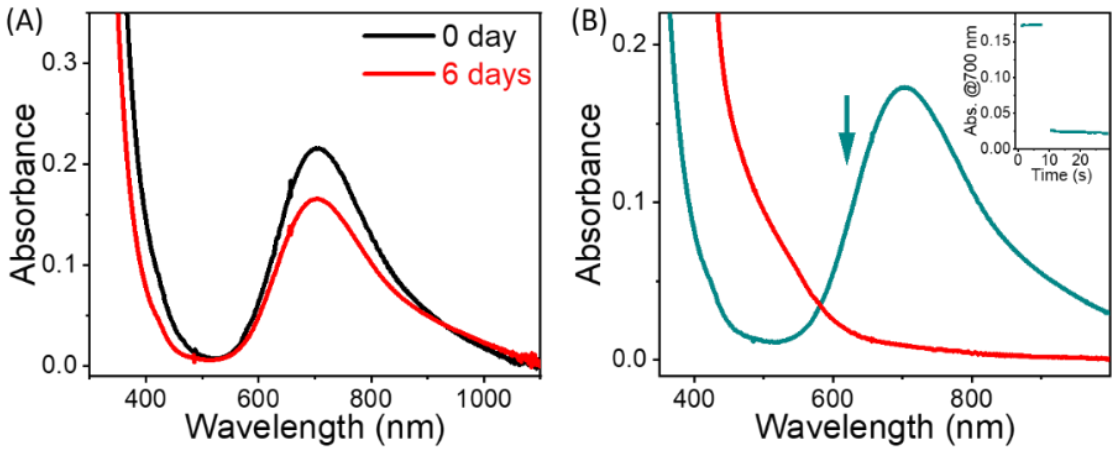

Figure S20: UV/Vis absorption changes depicting the (A) decay of **1**: (black) initial spectra and (red) after 6 days. (B) the instantaneous decay of **1** (solution kept for 6 days) upon addition of 20 eq. of phenol. Inset: The corresponding changes in the absorbance at 700 nm over time in seconds. *Conditions to generate **1**: 2 mM [Cu^{I}(NCCH$_3$)$_4$](ClO$_4$) in CH$_3$CN + 1 eq. of mCPBA at 25 ^{o}C.*

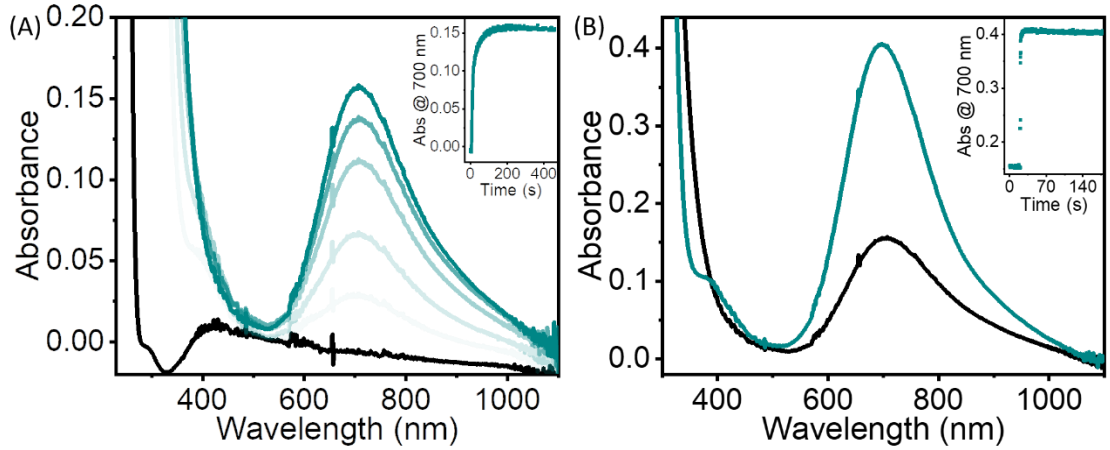

Figure S21: UV/Vis absorption changes depicting the reaction of (A) 2 mM [Cu^{I}(NCCH$_3$)$_4$](ClO$_4$) with 0.5 eq. of mCPBA at 25 ^{o}C. Inset: The corresponding changes in the absorption at 700 nm over time in seconds. (B) In continuation, to this 1.5 eq. of mCBA and 1.5 eq. of Et$_3$N (as a source of 3-chlorobenzoate) added. Inset: The corresponding changes in the absorption at 700 nm over time in seconds.

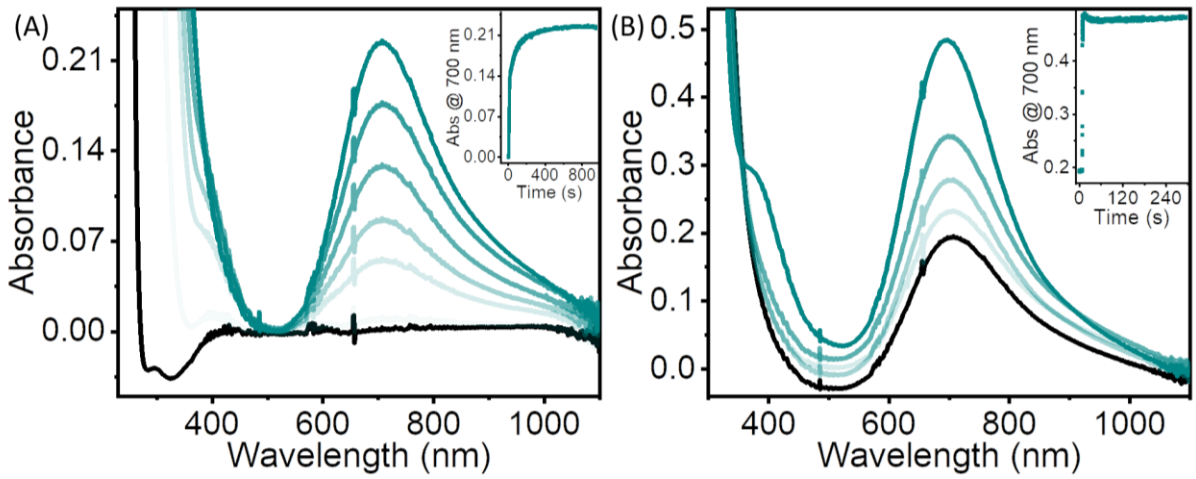

Figure S22: UV/Vis absorption changes depicting the reaction of (A) 2 mM $[Cu^{I}(NCCH_3)_4](ClO_4)$ with 1 eq. of mCPBA at 25 ^{o}C. Inset: The corresponding changes in the absorption at 700 nm over time in seconds. (B) In continuation, to this 1 eq. of mCBA and 1 eq. of Et_3N (as a source of 3-chlorobenzoate) added. Inset: The corresponding changes in the absorption at 700 nm over time in seconds.

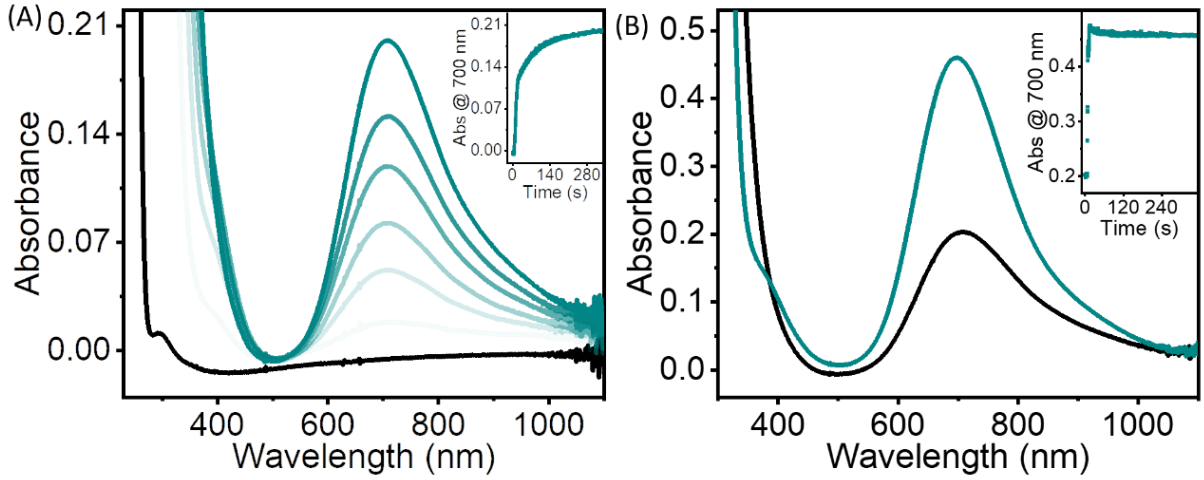

Figure S23: UV/Vis absorption changes depicting the reaction of (A) 2 mM $[Cu^{I}(NCCH_3)_4](ClO_4)$ with 1 eq. of mCPBA at 25 ^{o}C. Inset: The corresponding changes in the absorption at 700 nm over time in seconds. (B) In continuation, to this 1.5 eq. of mCBA and 1.5 eq. of Et_3N (as a source of 3-chlorobenzoate) added. Inset: The corresponding changes in the absorption at 700 nm over time in seconds.

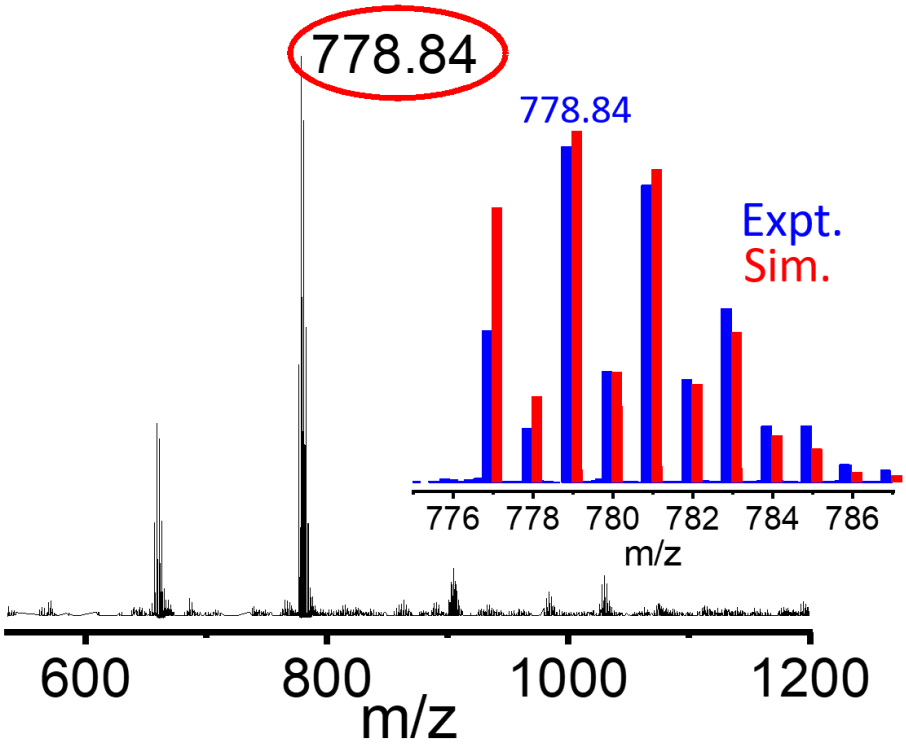

Figure S24: Negative mode ESI-mass spectrum of **2** in CH_3CN.

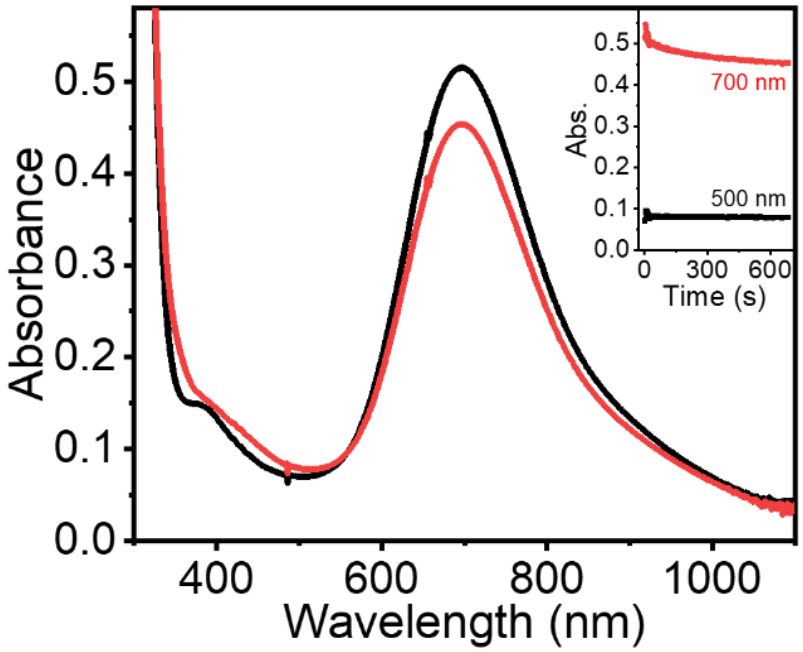

Figure S25: UV/Vis absorption changes depicting the reaction of 2 mM **2** (black) with 10 eq. of *p*-cresol. (red) Spectra recorded after 600 sec. of reactant added. Inset: The corresponding changes in the absorption at 700 nm and 500 nm over time in seconds. *Conditions to generate **2**: 2 mM $[Cu^{I}(NCCH_3)_4](ClO_4)$ + 0.5 eq. of mCPBA + 1.5 eq. of (mCBA + Et_3N) in CH_3CN at 25 ^{o}C.*

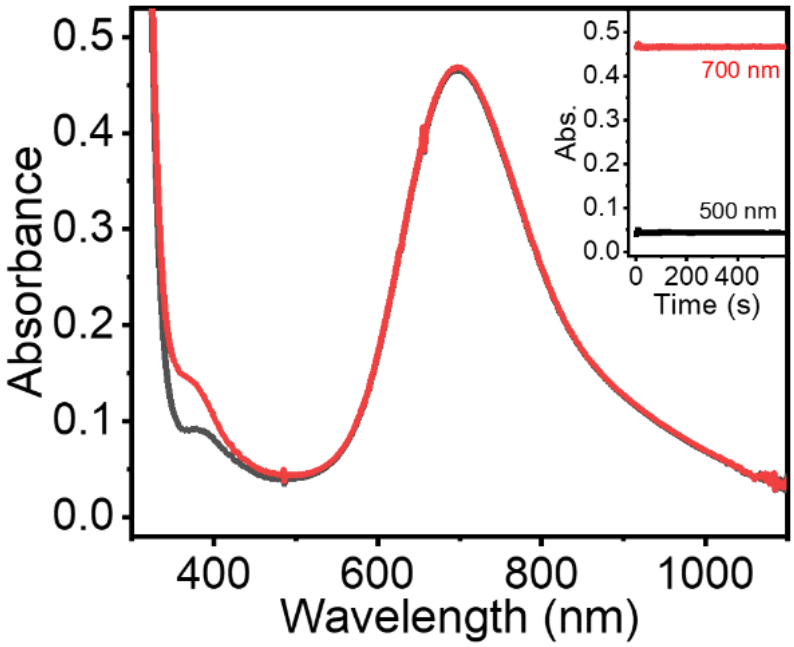

Figure S26: UV/Vis absorption changes depicting the reaction of 2 mM **2** (black) with 10 eq. of *p*-flurophenol. (red) Spectra recorded after 500 sec. of reactant added. Inset: The corresponding changes in the absorption at 700 nm and 500 nm over time in seconds. *Conditions to generate **2**: 2 mM [Cu^{I}(NCCH$_3$)$_4$](ClO$_4$) + 0.5 eq. of mCPBA + 1.5 eq. of (mCBA + Et$_3$N) in CH$_3$CN at 25 ^{o}C.*

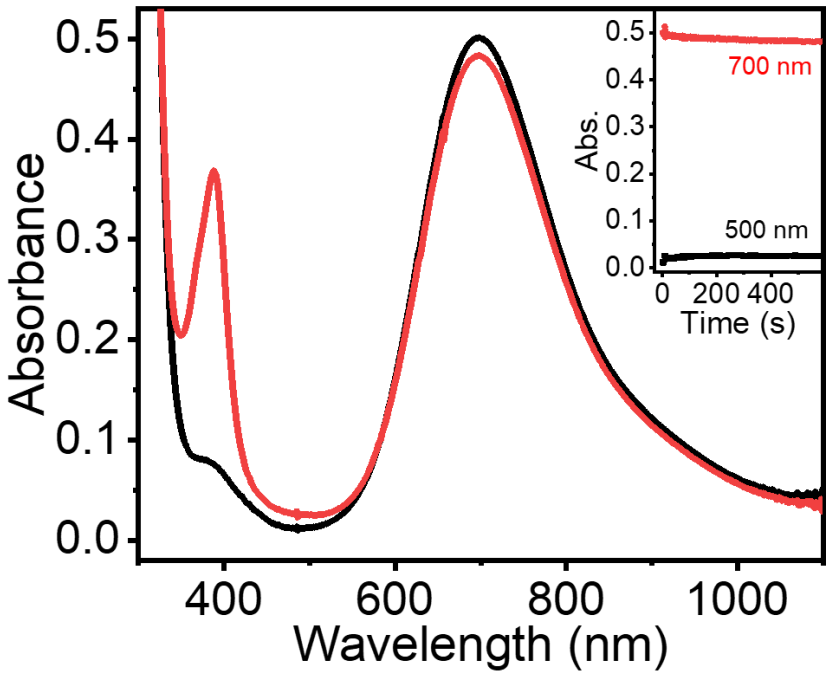

Figure S27: UV/Vis absorption changes depicting the reaction of 2 mM **2** (black) with 10 eq. of phenol. (red) Spectra recorded after 500 sec. of reactant added. Inset: The corresponding changes in the absorption at 700 nm and 500 nm over time in seconds. *Conditions to generate **2**: 2 mM [Cu^{I}(NCCH$_3$)$_4$](ClO$_4$) + 0.5 eq. of mCPBA + 1.5 eq. of (mCBA + Et$_3$N) in CH$_3$CN at 25 ^{o}C.*

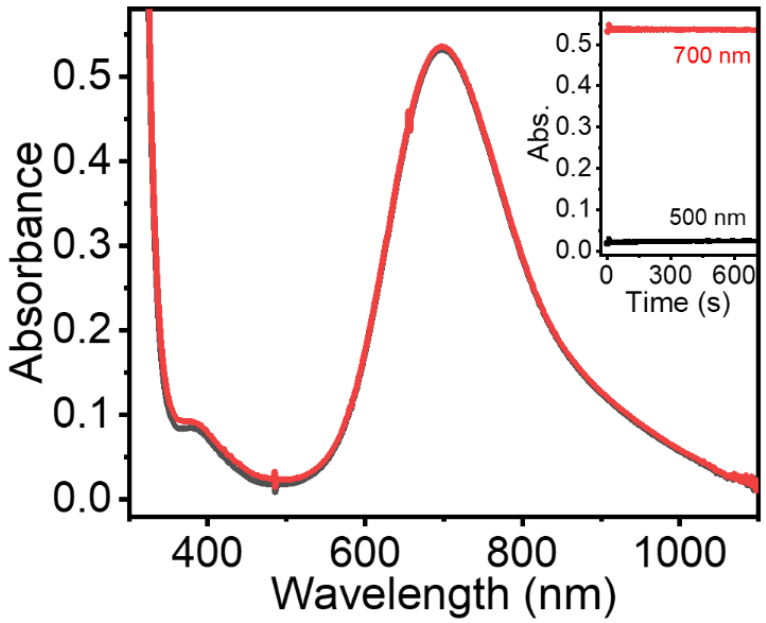

Figure S28: UV/Vis absorption changes depicting the reaction of 2 mM **2** (black) with 10 eq. of *p*-hydroxybenzonitrile. (red) Spectra recorded after 600 sec. of reactant added. Inset: The corresponding changes in the absorption at 700 nm and 500 nm over time in seconds. *Conditions to generate **2**: 2 mM [Cu^{I}(NCCH$_3$)$_4$](ClO$_4$) + 0.5 eq. of mCPBA + 1.5 eq. of (mCBA + Et$_3$N) in CH$_3$CN at 25 ^{o}C.*

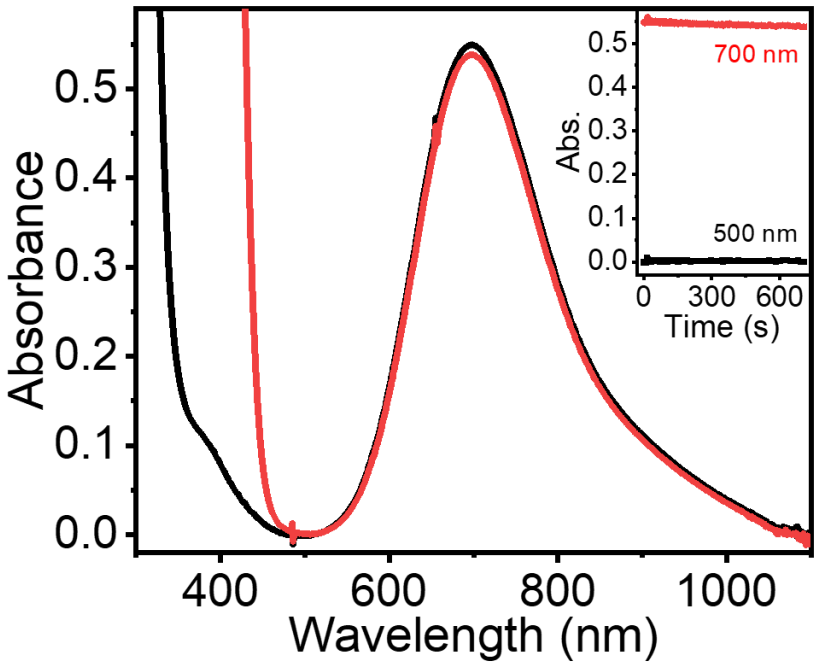

Figure S29: UV/Vis absorption changes depicting the reaction of 2 mM **2** (black) with 10 eq. of *p*-nitro phenol. (red) Spectra recorded after 600 sec. of reactant added. Inset: The corresponding changes in the absorption at 700 nm and 500 nm over time in seconds. *Conditions to generate **2**: 2 mM [Cu^{I}(NCCH$_3$)$_4$](ClO$_4$) + 0.5 eq. of mCPBA + 1.5 eq. of (mCBA + Et$_3$N) in CH$_3$CN at 25 ^{o}C.*

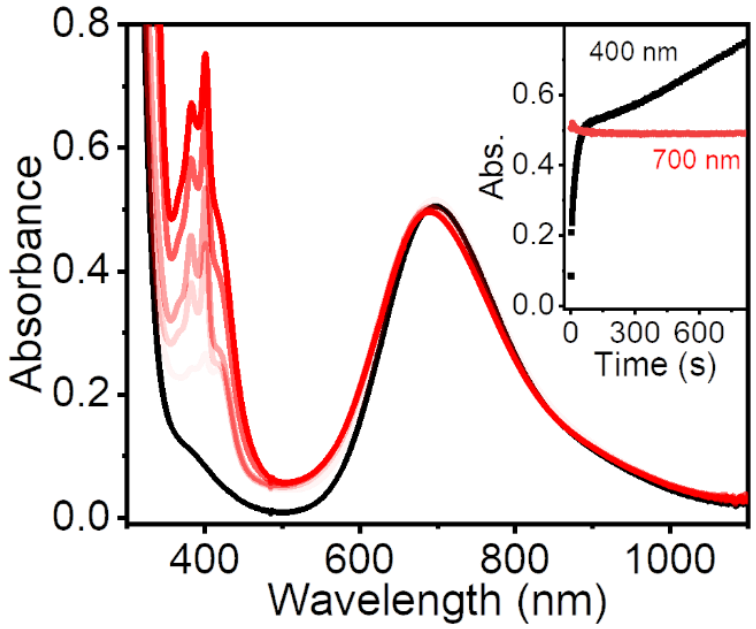

Figure S30: UV/Vis absorption changes depicting the reaction of 2 mM **2** with 2 eq. of 2,4,6-TTBP. Inset: The corresponding changes in the absorption at 700 nm and 400 nm over time in seconds. *Conditions to generate **2**: 2 mM [Cu^{I}(NCCH$_3$)$_4$](ClO$_4$) + 0.5 eq. of mCPBA + 1.5 eq. of (mCBA + Et$_3$N) in CH$_3$CN at 25 ^{o}C.*

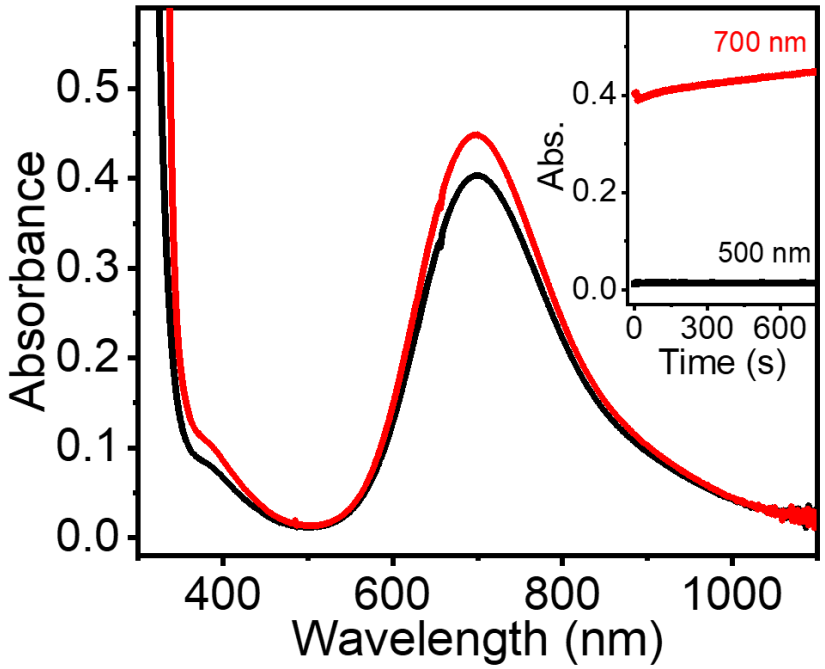

Figure S31: UV/Vis absorption changes depicting the reaction of 2 mM **2** (black) with 40 eq. of *2-PPA at 40 ^{o}C*. Inset: The corresponding changes in the absorption at 700 nm and 500 nm over time in seconds. *Conditions to generate **2**: 2 mM [Cu^{I}(NCCH$_3$)$_4$](ClO$_4$) + 0.5 eq. of mCPBA + 1.5 eq. of (mCBA + Et$_3$N) in CH$_3$CN at 40 ^{o}C.*

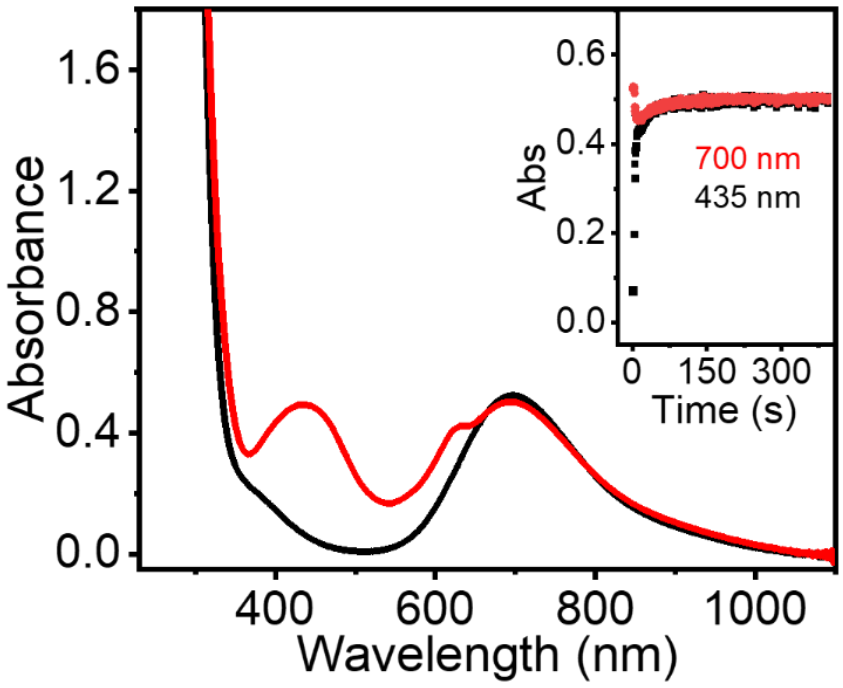

Figure S32: UV/Vis absorption changes depicting the reaction of 2 mM **2** with 2 eq. of ferrocene in CH_3CN. *Conditions to generate **2**: 2 mM $[Cu^{I}(NCCH_3)_4](ClO_4)$ + 0.5 eq. of mCPBA + 1.5 eq. of (mCBA + Et_3N) in CH_3CN at 25 ^{o}C.*

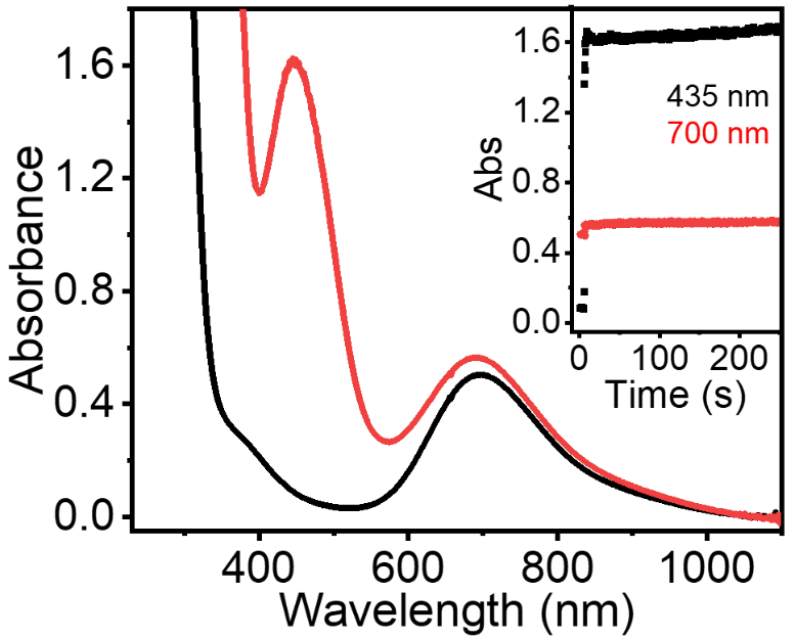

Figure S33: UV/Vis absorption changes depicting the reaction of 2 mM **2** with 2 eq. of acetylferrocene in CH_3CN. *Conditions to generate **2**: 2 mM $[Cu^{I}(NCCH_3)_4](ClO_4)$ + 0.5 eq. of mCPBA + 1.5 eq. of (mCBA + Et_3N) in CH_3CN at 25 ^{o}C.*

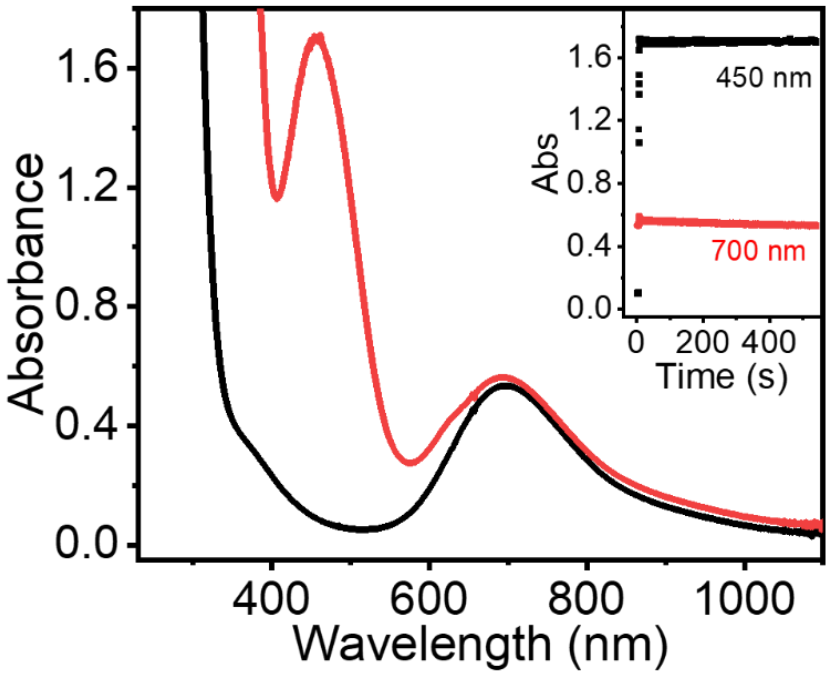

Figure S34: UV/Vis absorption changes depicting the reaction of 2 mM of **2** with 2 eq. of diacetyl ferrocene in CH_3CN. *Conditions to generate **2**: 2 mM $[Cu^{I}(NCCH_3)_4](ClO_4)$ + 0.5 eq. of mCPBA + 1.5 eq. of (mCBA + Et_3N) in CH_3CN at 25 ^{o}C.*

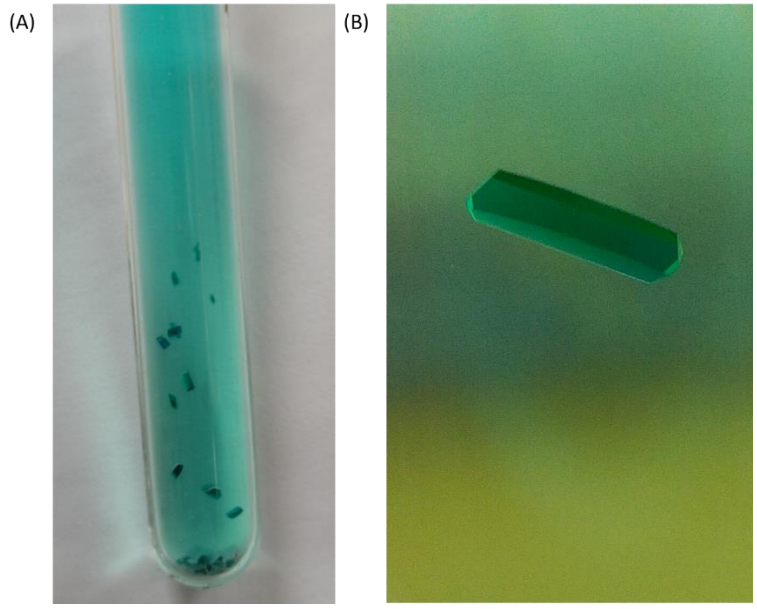

Figure S35: (A) Crystals of **2** formed by layering of hexane upon **1** in CH_3CN and (B) magnified view of a selected crystal.

Table S1: Crystal data and structure refinement of **2**.

Empirical formula	$C_{20}H_{17}Cl_2CuN_3O_4$
Formula weight	497.80
Temperature/K	100
Crystal system	triclinic
Space group	*P-1*
a/Å	10.1316(3)
b/Å	10.7203(3)
c/Å	11.9188(3)
α/°	68.1470(10)
β/°	68.4210(10)
γ/°	86.3640(10)
Volume/Å^3	1113.25(5)
Z	2
ρ_{calc}g/cm^3	1.485
μ/mm^{-1}	1.251
F(000)	506.0
Crystal size/mm^3	0.22 × 0.22 × 0.2
Radiation	MoKα (λ = 0.71073)
2Θ range for data collection/°	5.426 to 56.706
Index ranges	-13 ≤ *h* ≤ 13, -14 ≤ *k* ≤ 14, -15 ≤ *l* ≤ 15
Reflections collected	18162
Independent reflections	5560 [R_{int} = 0.0283, R_{sigma} = 0.0287]
Data/restraints/parameters	5560/0/293
Goodness-of-fit on F^2	1.080
Final R indexes [I>=2σ (I)]	R_1 = 0.0261, wR_2 = 0.0658
Final R indexes [all data]	R_1 = 0.0287, wR_2 = 0.0674
Largest diff. peak/hole / *e* Å^{-3}	0.52/-0.46

Table S2: Selected Bond lengths (Å) of **2**.

	Length/Å			**Length/Å**
Cu_1••••Cu_1^1	2.6483(3)		Cu_1—O_3	1.9583(10)
Cu_1—O_2^1	1.9716(11)		Cu_1—O_1	1.9657(10)
Cu_1—O_4^1	1.9706(10)		Cu_1—N_1	2.1675(13)

[1]1-X,1-Y,-Z

Table S3: Selected Bond Angles (Å) of **2**.

	Angle/˚		Angle/˚
O_2^1— Cu_1— Cu_1^1	83.18(3)	O_3— Cu_1 — O_4^1	168.19(4)
O_2^1— Cu_1— N_1	93.74(5)	O_1— Cu_1— O_2^1	168.33(4)
O_4^1— Cu_1— Cu_1^1	86.62(3)	N_1— Cu_1— Cu_1^1	175.13(4)
O_4^1— Cu_1 — O_2^1	89.37(5)	O_1— Cu_1— O_4^1	89.23(5)
O_4^1— Cu_1 — N_1	97.14(5)	O_1— Cu_1— N_1	97.93(5)
O_3— Cu_1— Cu_1^1	81.66(3)	O_3— Cu_1— N_1	94.64(5)
O_3— Cu_1— O_2^1	90.66(5)	O_1— Cu_1— Cu_1^1	85.17(3)
O_3— Cu_1— O_1	88.35(5)		

[1]1-X,1-Y,-Z

Table S4: Kinetic data for aldehyde deformylation of 2-phenylpropanaldehyde (2-PPA) with various 3d-metal based high valent intermediates at various temperatures.

Complex	k_2 [$M^{-1}s^{-1}$] (T [^oC])	Reference
1	0.0515 (40)	This work
$[Mn^{III}(O_2)(12\text{-TMC})]^+$	0.04 (20)	[1]
$[Mn^{III}(O_2)(13\text{-TMC})]^+$	0.03 (20)	[1]
$[Mn^{III}(O_2)(14\text{-TMC})]^+$	0.04 (20)	[1]
$[Mn^{III}(O_2)(Pro3Py)]^+$	0.003 (0)	[2]
$[Mn^{III}(N_3Py_2)(O_2)]^+$	0.16 (25)	[3]
$(BPMP)Mn^{II}\ Mn^{III}$ -peroxide	0.0006 (-90)	[4]
$[Mn^{III}(bispidine)(O_2)]^+$	0.0274 (15)	[5]
$[Fe^{III}(\eta_2\text{-OO})(TMC)]^+$	0.041 (15)	[6]
$[Fe^{III}(\eta_1\text{-OOH})(TMC)]^+$	0.13 (-40)	[7]
$[Co^{III}(\eta_2\text{-OO})(14\text{-TMC})]^+$	0.058 (0)	[8]
$[Co^{III}(\eta_2\text{-OO})(13\text{-TMC})]^+$	0.015 (25)	[8]
$[Co^{III}(\eta_2\text{-OO})(TMC)]^+$	0.058 (0)	[9]
$[Co^{III}(Me_3\text{-TPADP})(OO^tBu)_2]^+$	0.41 (25)	[10]
$[Ni^{III}(\eta_2\text{-OO})(TMC)]^+$	0.04 (25)	[11]
$(L_2)Ni^{II}$(superoxido)	0.00012 (25)	[12]
$[Ni^{III}(TBDAP)(O_2)]^+$	0.0074 (25)	[13]
$[Ni^{III}(CHDAP)(O_2)]^+$	0.062 (25)	[13]
$[Cu^{II}(CHDAP)(OOR)]^+$	0.12 (-40)	[14]
$(BPC)Cu^{II}(O\text{-}O^{-\bullet})$	0.062 (-80)	[15]
$[Cu^{II}(^iPr_3\text{-tren})(OOH)]^+$	0.15 (-50)	[16]

12-TMC = 1,4,7,10-tetramethyl-1,4,7,10-tetraazacyclododecane, 13-TMC = 1,4,7,10-tetramethyl-1,4,7,10-tetraazacyclotridecane, 14-TMC (or TMC) = 1,4,8,11-tetramethyl-1,4,8,11-tetraazacyclotetradecane, Pro3Py = 1-(pyridin-2-yl)-*N*-(pyridin-2-ylmethyl)-*N*-((1-(pyridin-2-ylmethyl)pyrrolidin-2-yl)methyl)methanamine, N_3Py_2 = *N*,*N'*-dimethyl-*N*-(2-(methyl(pyridin-2-ylmethyl)amino)ethyl)-*N'*-(pyridin-2-ylmethyl)ethane-1,2-diamine, HBPMP = 2,6-*bis*{[(*bis*(2-pyridylmethyl)amino]methyl}-4-methylphenol), bispidine = dimethyl 2,4-di(2-pyridyl)-3-benzyl-7-(pyridin-2-ylmethyl)-3,7-diazabicyclo[3.3.1] nonan-9-one-1,5-dicarboxylate, Me_3-TPADP = 3,6,9-trimethyl-3,6,9-triaza-1 (2,6)-pyridinacyclodecaphane, L_2 = Me*N*-(C(=O)NAr)$_2$; Ar=2,6-$^iPr_2C_6H_3$), TBDAP

= *N*,*N*'-di-*tert*-butyl-2,11-diaza[3.3](2,6)pyridinophane, CHDAP = *N*,*N*'-dicyclohexyl-2,11-diaza[3.3](2,6)pyridinophane, H_2BPC = *N*,*N*'-bis(2,6-diisoproylphenyl)-2,6-pyridinedicarboxamide, $^{i}Pr_3$-tren = tris[2-(isopropylamino)ethyl]amine.

References:

1 H. Kang, J. Cho, K. Bin Cho, T. Nomura, T. Ogura and W. Nam, *Chem. - A Eur. J.*, 2013, **19**, 14119–14125.

2 J. Du, D. Xu, C. Zhang, C. Xia, Y. Wang and W. Sun, *Dalt. Trans.*, 2016, **45**, 10131–10135.

3 D. D. Narulkar, A. Ansari, A. K. Vardhaman, S. S. Harmalkar, G. Lingamallu, V. M. Dhavale, M. Sankaralingam, S. Das, P. Kumar and S. N. Dhuri, *Dalt. Trans.*, 2021, **50**, 2824–2831.

4 A. M. Magherusan, S. Kal, D. N. Nelis, L. M. Doyle, E. R. Farquhar, L. Que and A. R. Mcdonald, *Angew. Chemie - Int. Ed.*, 2019, **58**, 5718–5722.

5 P. Barman, P. Upadhyay, A. S. Faponle, J. Kumar, S. S. Nag, D. Kumar, C. V. Sastri and S. P. de Visser, *Angew. Chemie - Int. Ed.*, 2016, **55**, 11091–11095.

6 J. Annaraj, Y. Suh, M. S. Seo, S. O. Kim and W. Nam, *Chem. Commun.*, 2005, 4529–4531.

7 J. Cho, S. Jeon, S. A. Wilson, L. V. Liu, E. A. Kang, J. J. Braymer, M. H. Lim, B. Hedman, K. O. Hodgson, J. S. Valentine, E. I. Solomon and W. Nam, *Nature*, 2011, **478**, 502–505.

8 Y. Jo, J. Annaraj, M. S. Seo, Y. M. Lee, S. Y. Kim, J. Cho and W. Nam, *J. Inorg. Biochem.*, 2008, **102**, 2155–2159.

9 Y. Jo, J. Annaraj, M. S. Seo, Y. M. Lee, S. Y. Kim, J. Cho and W. Nam, *J. Inorg. Biochem.*, 2008, **102**, 2155–2159.

10 B. Shin, Y. Park, D. Jeong and J. Cho, *Chem. Commun.*, 2020, **56**, 9449–9452.

11 J. Cho, R. Sarangi, J. Annaraj, S. Y. Kim, M. Kubo, T. Ogura, E. I. Solomon and W. Nam, *Nat. Chem.*, 2009, **1**, 568–572.

12 C. Panda, A. Chandra, T. Corona, E. Andris, B. Pandey, S. Garai, N. Lindenmaier, K. Silvio, E. R. Farquhar, J. Roithov, G. Rajaraman, M. Driess and K. Ray, *Angew. Chemie Int. Ed.*, 2018, **57**, 14883–14887.

13 J. Kim, B. Shin, H. Kim, J. Lee, J. Kang, S. Yanagisawa, T. Ogura, H. Masuda, T. Ozawa and J. Cho, *Inorg. Chem.*, 2015, **54**, 6176–6183.

14 B. Kim, D. Jeong and J. Cho, *ChemComm*, 2017, **53**, 9328–9331.

15 P. Pirovano, A. M. Magherusan, C. Mcglynn, A. Ure, A. Lynes and A. R. Mcdonald, *Angew. Chemie Int. Ed.*, 2014, **53**, 5946–5950.

16 B. Kim, D. Jeong, T. Ohta and J. Cho, *Commun. Chem.*, 2019, **2**, 1–6.